Studies of Interaction Mechanism Between Iron and HCN

Houzhang Tan*, Xuebin Wang, Yangqing Niu, Haiyu Liu,
Congling Wang and Tongmo Xu

*State Key Laboratory of Multiphase Flow in Power Engineering,
Xi'an Jiaotong University, Xi'an 710049, P.R. China
Fax: (86)(29)82668703; Tel: (86)(29)82665417; E-mail: tanhouzhang@yahoo.cn*

Interaction mechanism between iron and HCN has been investigated in a fixed bed, compared with calcium and magnesium and the original HCN is generated by pyridine pyrolysis. Results show that the interaction mechanism of HCN with Fe_2O_3 is totally different from CaO and MgO. Ferric oxide can transform HCN into NO, compared with that CaO and MgO convert HCN to N_2. Under the effect of Fe_2O_3, HCN begins to decrease at 473 K and when temperature is higher than 623 K, all HCN has been transformed. CH_4 starts to decrease linearly at around 348 K, disappearing at 623 K and CO increases continually from 348 K. The reaction between HCN and Fe_2O_3 is suggested as $2Fe_2O_3 + 3HCN \rightarrow 2Fe + 3CO + 3NO + 0.5H_2$. Iron formed in the reaction of HCN-Fe_2O_3 can further react with HCN to transform the nitrogen in HCN into N_2. Iron starts to reduce HCN from 423 K, when temperature is higher than 598 K, HCN has been converted completely and the nitrogen elements of N_2 are balanced with that of inlet HCN.

Key Words: HCN, Iron, FT-IR, NO, Temperature.

INTRODUCTION

Nitrogen oxides from coal combustion have induced acid rain and photochemical smog, continuing to be a significant threat against the environment[1,2]. It is also well known that during the process of coal combustion, most of nitrogen oxides are from fuel-N and HCN is considered as the predominant precursor of nitrogen oxides in the transformation from fuel-N to nitrogen oxides[3-5]. Therefore, the demonstration on the mechanism of HCN producing and converting is contributively to elucidating the root of nitrogen oxides generated and controlling the emission of nitrogen oxides during coal combustion.

Considerable studies have shown that in the process of coal pyrolysis or gasification, metal addition could affect the distribution of the nitrogenous species: HCN, NH_3 and N_2[1,6-16]. Long-term results of Ohtsuka and Tsubouchi[11,15] suggest that Ca^{2+} and Fe^{3+} ions catalyze the decomposition of HCN into N_2 and the effect of metal addition mass is not significant[7,15]. Zhao and Guan[17,18] also report that Fe, Ca and Na additions promote the transformation from fuel-N to N_2 and the load mode of iron strongly affect the catalytic effects of metal addition. Most of the results have

manifested metal addition catalytically transform HCN into N_2 and the metal additions are mainly corresponding to Na, Ca and Fe. In our previous research[16], the mechanism of interaction between calcium and HCN has been demonstrated, consistent with the results of Sachfer[12]. Nevertheless, the mechanism on reaction between iron and HCN is still unclear, due to the strong reducibility of iron and variety of its oxides many efforts have been performed.

The principal objective of the present study is to investigate the interaction mechanism between HCN and iron in different temperature range, compared with the reaction mechanism of HCN and calcium, magnesium. The original HCN was produced through the pyrolysis of pyridine and gaseous species (CO, HCN, H_2, CH_4 and N_2) are quantitatively detected by Fourier transform infrared gas analyzer (GA) coupled with gas chromatography (GC).

EXPERIMENTAL

HCN preparation (pyrolysis of pyridine): Restricted by complex structures of coal and catalysis of mineral matters, it is difficult to obtain precise transformation mechanism of coal nitrogen directly, thus many works have been performed with model compounds, including pyridine[19-23], pyrrole[24-27]. In the pyrolysis of the model compounds, HCN is generally believed to be the most important nitrogen-containing product[19-23].

In this work, pyridine (C_5H_5N) has been chosen as the source of HCN and pyrolysis of pyridine was presented in quartz reactor-A at 1273 K. As shown in Fig. 1,
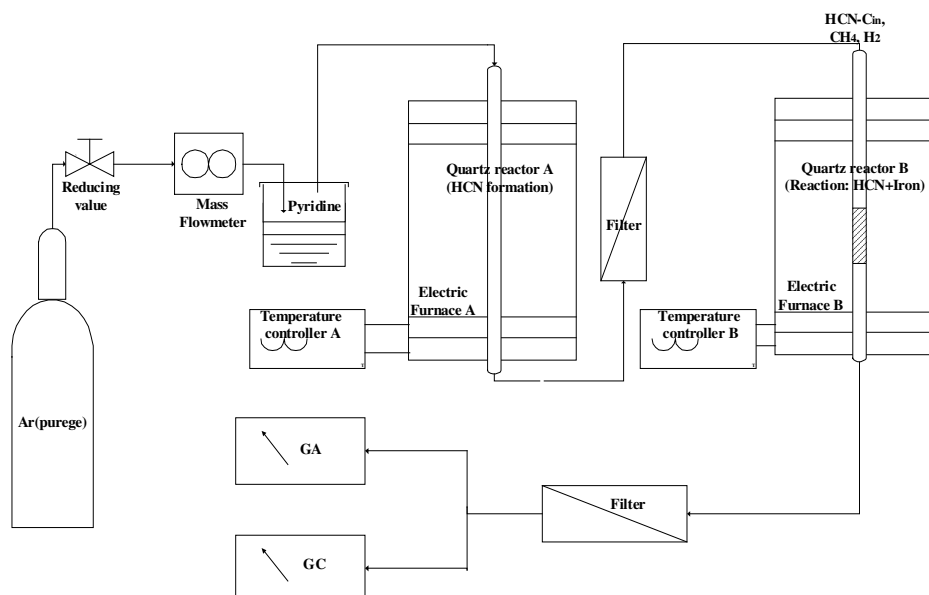

Fig. 1. Schematic diagram of experimental system for HCN formation and removal

volatile pyridine in vessel was carried out by the blowing of high-purity argon (> 99.999 %) into reactor-A and the flow rate of argon was controlled stable at 600 mL min^{-1} by mass flow meter. Long-time detection for HCN and CH$_4$ after quartz reactor-A has proved that the yields of gaseous species are stable and pyrolysis of pyridine can provide reliable HCN for the followed experiment of HCN-iron reaction in reactor-B.

Interaction between HCN and iron: The interaction experiment between HCN and iron was carried out in reactor-B, 20 mm in inner diameter and 1000 mm in length and the constant-temperature heating zone was longer than 600 mm. Ferric oxide (Fe$_2$O$_3$) or pure-iron (Fe) powders were placed on an orifice in the middle of reactor and it was squeezed in the mold at 5 MPa for 5 min, then crushed and sieved to 1.0-1.7 mm and the stacking thickness of powders on the orifice is kept constant at 12 mm. It undergoes a process of temperature programmed reaction and the temperature increases to 1273 K with a heating rate of 10 K min^{-1}. Gas analyzer on-line monitored the gas species (HCN, CH$_4$, CO, NO), meanwhile, at several typical temperature, GC is used to quantify the concentration of N$_2$ and H$_2$.

All the gaseous products *i.e.*, HCN, CO and CH$_4$ were detected by DX-4000 gas analyzer (1.07 L gas analysis cell with a path of 5 m, resolution of 8 cm^{-1}, response time < 120 s, wave-number range of 4200-900 cm^{-1} and scan frequency of 10 spectra s^{-1}). The lowest detectable concentration was 1ppm and the estimated uncertainly limits of measurements were within ± 2 %. Agilent-9800 GC (thermal conductivity detector, stationary phase of 5A molecule sieve, carrier gas of argon, column of 4 mm × 5 m, column temperature of 341 K) was used to quantify the concentration of H$_2$ and N$_2$.

RESULTS AND DISCUSSION

Effect of temperature on interaction between HCN and Fe$_2$O$_3$ compared with CaO and MgO: Fig. 2 illustrates the profile of gaseous species on-line detected by FTIR gas analyzer, during the process of temperature programmed reaction. Compared the results of HCN-Fe$_2$O$_3$ (Fig. 2a) and HCN-MgO (Fig. 2b), it is implied that the reaction mechanism with HCN is totally different. In the temperature programmed process, the decrease of HCN only displays one stage for Fe$_2$O$_3$ with the evolution of NO and considerable CO, compared with a profile of two stages for MgO without NO and less CO.

As seen from Fig. 2a, under the effect of Fe$_2$O$_3$, the concentration of HCN begins to decrease at 473 K, corresponding to the increase of NO. When temperature is higher than 623 K, all HCN has been transformed and the concentration of NO begins to keep constant. Methane starts to decrease linearly at around 348 K, disappearing at 623 K. Along with the change of CH$_4$, CO increases continuously from 348 K until 1273 K.

Comparably, the gaseous species profile of HCN-MgO is similar to that of HCN-CaO, which has been demonstrated in our previous research[16]. However, seen
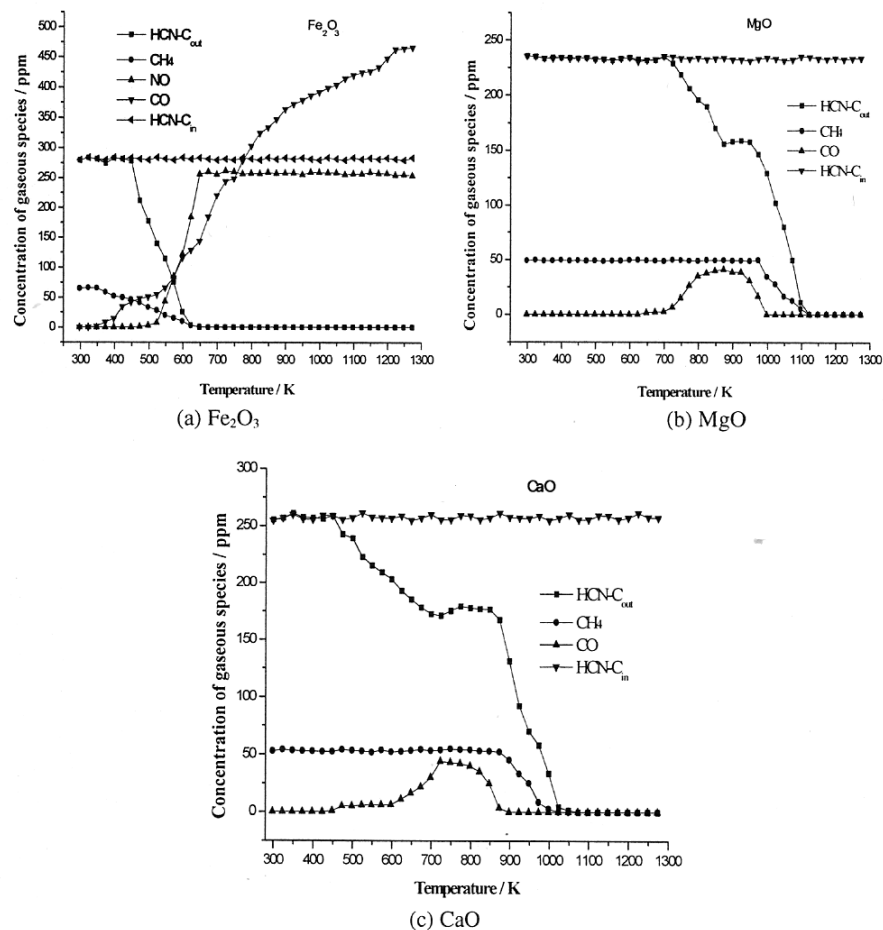
(a) Fe$_2$O$_3$

(b) MgO

(c) CaO

Fig. 2. Comparison of gaseous species detected on-line after the reaction of HCN with metal oxides

from the Fig. 2b, the reactivity for HCN removal by MgO is weaker than CaO. Under the catalysis of MgO, the start temperature of HCN reduced has risen up to 723 K and the temperature for CaO is 473 K. The temperature difference is mainly focus on the first stage of HCN removal, when temperature has risen up to the second stage, both MgO and CaO reduced the concentration of HCN to zero and the difference of ending temperature is only 50 K.

Table-1 shows the comparison of the effect of Fe$_2$O$_3$, MgO and CaO on the profile of gaseous species including H$_2$ and N$_2$ at three temperatures. Considerable H$_2$ is mainly from the pyrolysis of pyridine and increases with temperature increasing. At lower temperature 723 K, the concentration of N$_2$ has kept constant for Fe$_2$O$_3$, but the test conditions for MgO and CaO detected no N$_2$ and N$_2$ is not detected until

1123 K and 923 K for MgO and CaO, respectively. At these three temperatures, HCN and CH_4 has disappeared for the reaction of Fe_2O_3, however, for the reaction of MgO and CaO, CH_4 decreases combined the beginning of the second stage of HCN removal and the ending temperature of HCN disappearing is around 1050 K.

TABLE-1
PROFILES OF GASEOUS SPECIES AT THREE TEMPERATURES

Additions	Temperature (K)	HCN-C_{in} (ppm)	Concentration of outlet-components (ppm)				
			HCN	CH_4	H_2	N_2	CO
Fe_2O_3	723	279.6	0	0	765.0	22.56	257
	923	279.6	0	0	856.5	22.13	378
	1123	279.6	0	0	977.4	23.15	431
MgO	723	235.4	229.00	50.0	525.0	0	7
	923	235.4	159.10	53.0	573.0	0	41
	1123	235.4	0	0	886.0	124.9	0
CaO	723	255.3	171.12	56.0	561	0	43
	923	255.3	92.14	37.5	839	83.0	0
	1123	255.3	0	0	918	137.0	0

Possible mechanism of HCN-Fe_2O_3 interaction: In our previous studies, we have demonstrated the mechanism of HCN removal by CaO. It is found that during the two temperature stages of HCN removal, the reaction mechanism is different, at a lower temperature HCN is removed by the route: $CaO + 2HCN \rightarrow CaCN_2 + CO + H_2$; but at higher temperatures, CaO removes HCN by another catalytic route: $2C_iH_j + 2HCN \rightarrow N_2 + (j + 1 - k)H_2 + 2C_i + 1H_k$. As seen from Fig. 2b and 2c, the profile of gaseous species with temperature is similar for MgO and CaO. Thus, it is suggested that the interaction mechanism of MgO and HCN: at temperature lower than 923 K, HCN is removed by MgO through the route: $MgO + 2HCN \rightarrow MgCN_2 + CO + H_2$; but when temperature is higher than 973 K, it is a catalysis route consuming hydrocarbon.

Fig. 2 has shown that the mechanism of HCN-Fe_2O_3 is totally different with CaO and MgO and it illustrates most of the nitrogen element in HCN has been transformed into NO, because in this experiment HCN is the only source of nitrogen, then NO must be the product of HCN reduced by Fe_2O_3. Thus, there is still a small part of nitrogen undetected and where is the residual nitrogen? Concentration of N_2 from GC is shown in Table-1 and Fig. 3, the sum of nitrogen in N_2 and NO is approximately equal to the nitrogen in HCN reduced and the nitrogen mass in gas species (HCN, NO and N_2) is balanced at temperature higher than 473K.

Meanwhile, there is no H_2O and CO_2 detected in the process and the reaction between HCN and Fe_2O_3 is supposed as: $2Fe_2O_3 + 3HCN \rightarrow 2Fe + 3CO + 3NO + 0.5H_2$. The Gibbs free energy change ΔG and enthalpy change ΔH of the reaction are calculated as -717.6 kJ mol^{-1} and -78.4 kJ mol^{-1}, therefore, the assumed reaction is able to occur and its reaction rate increases with temperature increasing.
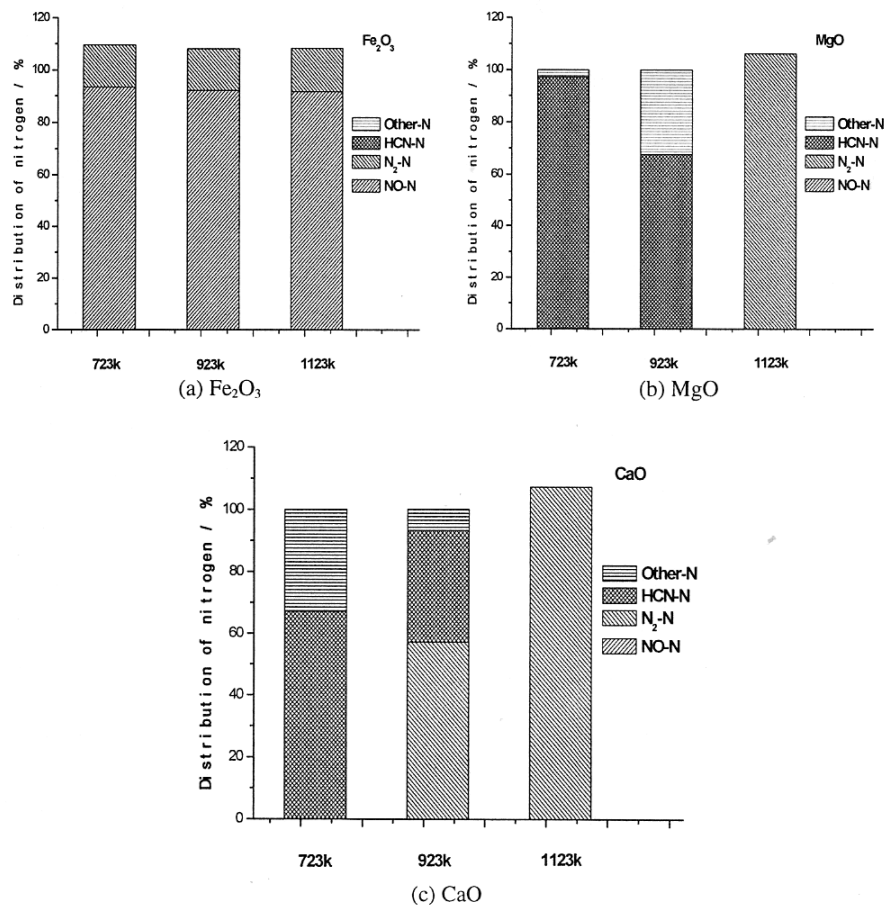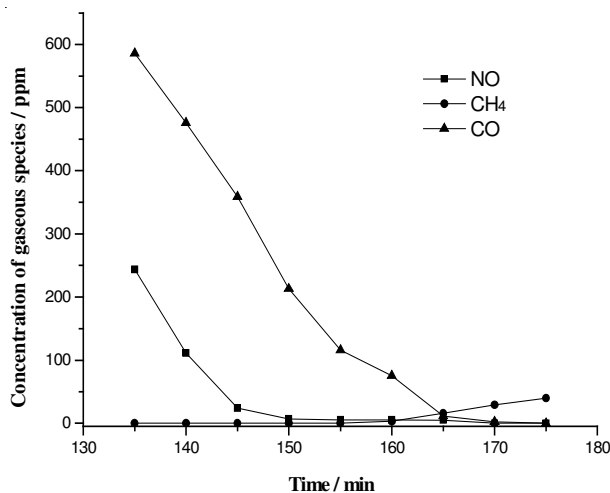
(a) Fe_2O_3

(b) MgO

(c) CaO

Fig. 3. Distribution of nitrogen element in different species at three temperatures

Indeed, GC has detected N_2, which may be the product of reaction of HCN with pure Fe formed at later stage. Fig. 4 provides the gaseous species profile after 135 min in isothermal experiments at 1273 K. It shows that after a long period of reaction, most of Fe_2O_3 has been transformed and the concentration of NO and CO gradually decreases to zero, which illustrates the reaction of HCN-Fe_2O_3 has stopped. However, the concentration of HCN is still kept at zero; thus, it should be due to the interaction of pure Fe formed after the reaction. When NO and CO disappears, CH_4 begins to be re-detected.

Table-2 and Fig. 5 have shown the concentration of N_2 and distribution of nitrogen element after 130 min. It also demonstrates that with the continuance of HCN-Fe_2O_3 reaction, the concentration of N_2 increases gradually to keep stable and the nitrogen mass is approximately balanced between HCN of inlet and NO/N_2 of outlet.

Fig. 4. Gas species monitored by GA after 135 min during the reaction HCN-Fe₂O₃

TABLE-2
PROFILES OF GASEOUS AT THREE TYPICAL TIMES

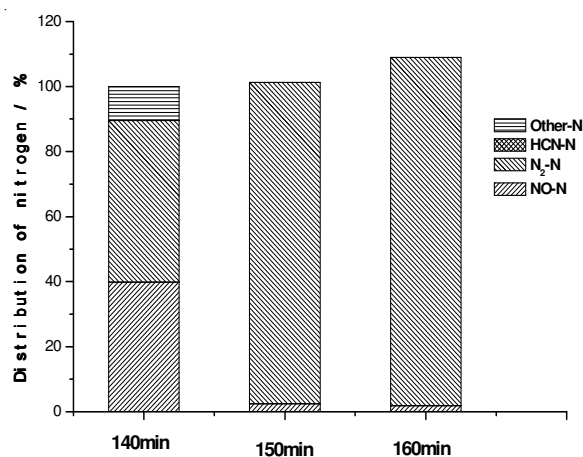| Time (min)	CH$_4$ (ppm)	H$_2$ (ppm)	N$_2$ (ppm)	CO (ppm)
140	0	1011.0	69.5	631
150	0	992.0	138.2	124
160	9.13	968.7	149.8	0

Fig. 5. Distribution of nitrogen element after 130 min

Verification of the result of HCN-Fe reaction: To further certificate the role of pure Fe on HCN reduction, the experiment of HCN-Fe has been performed undergoing the same process as metal oxides mentioned before. Fig. 6 shows the gaseous species profile detected online by FTIR gas analyzer, it can be seen that HCN begins to be reduced from 423 K and disappeared rapidly from 598 K, however, the concen-

tration CH_4 dose not change and there is no CO and NO generated. The profile of N_2 concentration can be seen from Table-3, which shows that its concentration is kept constant at around 147 ppm. The inlet HCN concentration is 281 ppm, thus the nitrogen in N_2 is equal to that in inlet HCN, which suggests that all the nitrogen in HCN has been transformed into N_2 under the reaction of pure Fe.
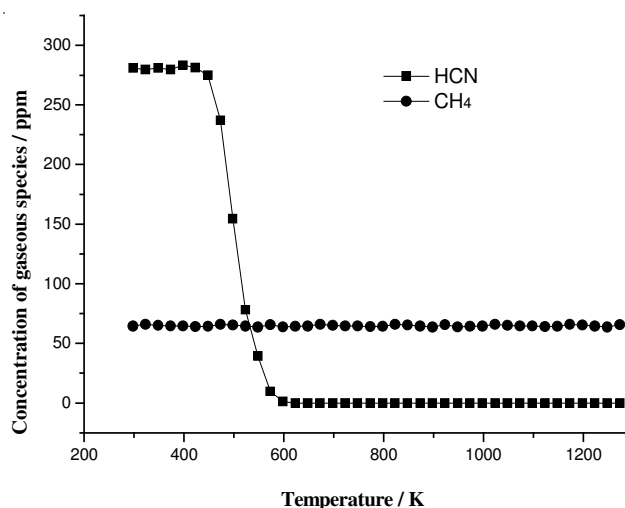

Fig. 6. Profile of HCN and CH_4 with temperature during the reaction HCN-Fe

TABLE-3
PROFILES OF GASEOUS SPECIES AT THREE TYPICAL
TEMPERATURES DURING THE REACTION HCN-Fe

Additions	Temperature (K)	HCN-C_{in} (ppm)	Concentration of outlet-components (ppm)			
			HCN	CH_4	H_2	N_2
	723	281.1	0	68.00	793.6	146.9
Fe_2O_3	923	281.1	0	66.90	879.2	148.2
	1123	281.1	0	66.92	981.5	147.2

Conclusion

The interaction mechanisms between HCN and iron were investigated compared with calcium and magnesium and the original HCN was generated by pyrolysis of pyridine. Conclusions are summarized below: (1) The interaction mechanism of HCN-Fe_2O_3 is totally different with HCN-CaO and HCN-MgO and Fe_2O_3 can transform HCN into NO, compared with that CaO and MgO convert HCN to N_2. Under the effect of Fe_2O_3, HCN begins to decrease at 473 K and when temperature is higher than 623 K, all HCN has been transformed. CH_4 starts to decrease linearly at around 348 K, disappearing at 623 K and CO increases continuously from 348 K. The reaction between HCN and Fe_2O_3 is suggested as $2Fe_2O_3 + 3HCN \rightarrow 2Fe + 3CO + 3NO + 0.5H_2$. (2) Iron formed in the reaction of HCN-Fe_2O_3 can further

react with HCN to transform the nitrogen in HCN into N_2. Fe starts to reduce HCN from 423 K, when temperature is higher than 598 K, HCN has been converted completely and the nitrogen elements of N_2 are balanced with that of inlet HCN.

ACKNOWLEDGEMENT

REFERENCES

1. Y. Ohtsuka, H. Mori, K. Nonaka, T. Watanabe and K. Asami, *Energy Fuels*, **7**, 1095 (1993).
2. J.M. Beer, *Progr. Energy Combustion Sci.*, **26**, 301 (2000).
3. S.C. Hill and L.D. Smoot, *Progr. Energy Combustion Sci.*, **26**, 417 (2000).
4. P. Glarborg, A.D. Jensen and J.E. Johnsson *Progr. Energy Combustion Sci.*, **29**, 89 (2003).
5. P. Dagaut, P. Glarborg and M.U. Alzueta, *Progr. Energy Combustion Sci.*, **34**, 1 (2008).
6. J.-I. Hayashi, K. Kusakabe, S. Morooka, M. Nielsen and E. Furimsky, *Energy Fuels*, **9**, 1028 (1995).
7. H. Mori, K. Asami and Y. Ohtsuka, *Energy Fuels*, **10**, 1022 (1996).
8. A. Jensen, J.E. Johnsson and K. Dam-Johansen, *AIChE J.*, **43**, 3070 (1997).
9. Y. Ohtsuka, W. Zhiheng and E. Furimsky, *Fuel*, **76**, 1361 (1997).
10. Y. Ohtsuka, T. Watanabe, K. Asami and H. Mori, *Energy Fuels*, **12**, 1356 (1998).
11. N. Tsubouchi, Y. Ohshima, C. Xu and Y. Ohtsuka, *Energy Fuels*, **15**, 158 (2001).
12. S. Schäfer and B. Bonn, *Fuel*, **81**, 1641 (2002).
13. M.-Y. Xu, Y.-P. Cui, L.-L. Qin, L.-P. Chang and K.-C. Xie, *J. Fuel Chem. Technol.*, **35**, 5 (2007).
14. H.-F. Liu, Y.-H. Liu, Y.-H. Liu and D.-F. Che, *J. Fuel Chem. Technol.*, **36**, 134 (2008).
15. N. Tsubouchi and Y. Ohtsuka, *Fuel Processing Technol.*, **89**, 379 (2008).
16. H. Tan, X. Wang, C. Wang and T. Xu, *Energy Fuels*, **23**, 1545 (2009).
17. Z. Zhao, W. Li and B. Li, *Fuel*, **81**, 1559 (2002).
18. R. Guan, W. Li, H. Chen and B. Li, *Fuel Processing Technol.*, **85**, 1025 (2004).
19. A.E. Axworthy, V. H. Dayan and G.B. Martin, *Fuel*, **57**, 29 (1978).
20. J.C. Mackie, M.B. Colket and P.F. Nelson, *J. Phys. Chem.*, **94**, 4099 (1990).
21. J.H. Kiefer, Q. Zhang, R.D. Kern, J. Yao and B. Jursic, *J. Phys. Chem. A*, **101**, 7061 (1997).
22. Y. Ninomiya, Z. Dong, Y. Suzuki and J. Koketsu, *Fuel*, **79**, 449 (2000).
23. H.U.R. Memon, K.D. Bartle, J.M. Taylor and A. Williams, *Int. J. Energy Res.*, **24**, 1141 (2000).
24. A. Lifshitz, C. Tamburu and A. Suslensky, *J. Phys. Chem.*, **93**, 5802 (1989).
25. J.C. Mackie, M.B. Colket, P.F. Nelson and M. Esler, *Int. J. Chem. Kinetics*, **23**, 733 (1991).
26. M. Martoprawiro, G.B. Bacskay and J.C. Mackie, *J. Phys. Chem. A*, **103**, 3923 (1999).
27. L. Zhai, X.F. Zhou and R.F. Liu, *J. Phys. Chem. A*, **103**, 3917 (1999).